AN IN VIVO MODEL FOR THE ACUTE RESPONSE OF NEURAL TISSUE TO TRAUMATIC LOADING

Kenneth A. Barbee, Joseph Yazdi[†], Babak Abai[†], Sydney Croul[†], Robert Fijan[*], and Lawrence E. Thibault

Drexel University, Philadelphia, PA USA
[†]Medical College of Pennsylvania & Hahnemann University of the Health Sciences, Philadelphia, PA USA
[*]Exponent Failure Analysis Associates, Inc., Philadelphia, PA USA

ABSTRACT

The Guinea Pig optic nerve stretch was developed as an in vivo model for central nervous system trauma. This model allows a controlled dynamic stretch to be applied to a single nerve tract with a specific set of physiological functions. Thus, the mechanical stimulus can be related directly to the resulting tissue dysfunction. However, because of the system's configuration, there are some simple, but not trivial, mechanical considerations that will strongly influence the interpretation of results from this model, especially with regard to the establishment of injury tolerance criteria. Thus, we performed a detailed study of the structural mechanics of the system the globe, optic nerve, muscle and connective tissues, and their attachments to the skull and other structures. Results from these studies allowed us to determine an appropriate pre-load for subsequent dynamic injury experiments. Stretches of 25% applied over 10 milliseconds reliably produced acute swelling of axons of sufficient magnitude to be observed by light microscopy with toludine blue staining. The degree of swelling reaches a peak at 4 hours post injury. These results set the stage for subsequent tests of treatments designed to intervene in the cascade of events initiated by the primary mechanical trauma.

CENTRAL NERVOUS SYSTEM (CNS) injury due to trauma is a significant cause of mortality and long-term morbidity worldwide. Much research has been done in the recent years in order to elucidate the mechanism and pathophysiology of traumatic brain injury (TBI). To this effort, numerous cell culture and animal models have been designed. Work in our laboratory and others has suggested that acute mechanical disruption of cell membrane may cause transient phenomena that lead to the secondary sequelae of neural injury (Barbee, 1998; Galbraith, 1993; Ellis, 1995). In our laboratory, we have developed a cell culture model for neuronal injury in which the injury mechanisms and candidate pharmacological interventions can be tested. However, in order to advance to a preclinical trial of candidate pharmacological therapies, an *in vivo* model is essential. From the biomechanical point of view, the CNS is extremely complex. Therefore, the best approach is a simple model of axonal deformation with the added complexity of an *in vivo* tissue model. The goal with this model is to develop a

system in which all parameters are known and can be controlled so that the injury may be precisely reproduced, and even more importantly, pharmacological agents can be tested accurately.

We have previously described an *in vivo* guinea pig optic nerve stretch model which produces injury that resembles the morphological changes seen in human diffuse axonal injury (DAI) (Gennarelli *et al.*, 1989). This and subsequent studies (Jafari, 1997, 1998; Maxwell, 1995, 1997) showed short- and long-term pathological morphology of axons in response to the imposed trauma. However, these were rather mild injuries requiring electron microscopy to make accurate measurements of subtle changes in axonal dimension. Nevertheless, there are important advantages to this model over other animal models previously described. The anatomy and function of the optic nerve are discrete and have been well studied. The stretch injury correlates well with the mechanism of injury encountered in DAI. Although this model is geometrically simple, there are some uncertainties in the mechanics, specifically in the manner in which force is transmitted through the optic nerve as well as selection of appropriate gauge length for calculating nerve strain. Thus, we undertook to make certain modifications to this system. First, we performed a detailed anatomical dissection of the entire system, which gave us a greater understanding of the structures involved. Static and dynamic stretches were applied, and direct measurements of optic nerve deformation were made. We were also able to demonstrate significant injury consistently. Therefore, by controlling the loading parameters, we can produce injuries that correlate well with all degrees of axonal injury. With the increased injury severity achievable with our new model, we can study the effects of stretch injury under light microscopy acutely thus bypassing the cumbersome and time-consuming technique of electron microscopy on a large number of specimens. Our model is simple yet versatile so that it can easily lend itself to the study of axonal injury utilizing various methods such as electrophysiology and molecular biology. Moreover, this model can be modified for the use of pharmacological agents in the treatment of DAI.

MATERIALS AND METHODS

ANIMAL PREPARATION: Adult albino guinea pigs, ranging in weight from 500-1000 grams, were utilized in this study. The guinea pigs were anesthetized with intraperitoneal injection of ketamine 87 mg/kg and xylazine 13 mg/kg. With the aid of an operating microscope, the conjunctiva and the extraocular muscles of the right eye were dissected sharply from the sclera, and the optic nerve was exposed at the posterior pole of the globe. From this point forward, the optic nerve and chiasm were bathed in normal saline solution at all times. At this junction, there were two types of dissections. The first set involved a limited resection of the orbital roof and surrounding soft tissue only at the region near the globe so that the structures at the optic foramen were not disturbed. The second type consisted of removal of all bony and connective tissue components along the entire length of the optic nerve so that it was completely free of all attachments to the skull. In either configuration, the length of the optic nerve from the globe to the chiasm was measured.

QUASISTATIC LOADING: A sling fashioned from umbilical tape was made with an opening in the middle to accommodate the globe. The sling was positioned firmly against the posterior pole of the globe so that only the optic nerve ran through the slit. The sling was then pulled over a pulley and secured to an apparatus so that it could accommodate various weights. Quasi-static load-deflection tests were performed on the optic nerve in each dissection type above. To assess the contribution of the connective tissue sheath and its attachment to the foramen, the quasi-static loading experiment was repeated with the following modifications: the optic foramen was kept intact, but the optic nerve was sharply sectioned at the level of the chiasm. The specimens were kept at the desired lengths and fixed *in situ* with 1% gluteraldehyde in 4% paraformaldehyde solution for two hours. The optic nerves were sectioned *en block* and re-measured to assure that their lengths did not decrease as a result of their recoil capacity of inadequate fixation. Further preparation of the tissue for microscopic examination is described below.

DYNAMIC LOADING: We then turned our focus to studying the anatomical and morphological changes seen in the optic nerve under dynamic loading. The guinea pigs were anesthetized and their right optic nerves dissected as outlined above making certain that the connective tissue at the orbital foramen remained intact. The guinea pigs were then mounted onto our dynamic stretch apparatus which consisted of a pair of ear bars and a mouth piece in order to immobilize the skull. The motor that produced the stretch was placed at about forty-five degrees from the midline. This was based on our findings from earlier anatomical dissections which showed this to be the angle at which the nerve passed through the optic foramen. A Zeta stepper motor (Compumotor, CA) was used to apply the dynamic deformation. A Microsoft Windows-based program, Compumotor 6000, was operated as an interface between user and the control system. This configuration allows the experimenter to input user-defined displacement profiles into the computer, load them into the Zeta controller unit and then send the information out to the stepper motor. The motor has a velocity accuracy of ±0.02% of the maximum rate, thus increasing the accuracy of the prescribed loading conditions.

Both the length of the stretch as well as the time interval for the stretch were controlled independently. All stretches occurred during a ten millisecond interval. In order to have uniform tension in the sling of all specimens, a preload resulting in a 3-5% strain of the optic nerve was utilized. This was based on our biomechanical analysis of the quasi-static loading experiments. The optic nerves then underwent a 25% strain. This corresponded to a moderate or severe level of injury, respectively. The specimens were fixed at 0, 2, 4, or 6 hours after injury *in situ* in 1% gluteraldehyde in 4% paraformaldehyde solution for two hours. The contralateral optic nerve of those specimens fixed at six hours were also fixed at the same time in order to acount for any systemic, including anesthetic, effects on the optic nerves.

HISTOLOGY: Following the initial in situ fixation, the specimens were then cut at the chiasm and removed *en block* with the globe attached in order to maintain proper orientation of the nerve. They were further fixed *in vitro* for an additional twenty-four hours in the same solution. The specimens were then

gradually dehydrated with graded alcohols and embedded in epoxy resin. During this stage, the orientation of the optic nerves was preserved so that the portions closest to the chiasm could be studied separately from those in the middle or closest to the globe. Each block was then cut into one-micron thick slices. The morphology of each specimen was studied under light microscopy. Specifically, the undulatory pattern of the nerves at various strains in the longitudinal sections as well as the axonal diameters in the cross sections were compared.

In order to trace individual axons within the tissue matrix, a novel fluorescent labeling technique was used. The fluorescent, lipophilic, carbocyanine tracer DiI (1,1'-dioctadecyl-3,3,3',3'-tetramethylinso-carbocyanine perchlor-ate) was injected into the cut end of the nerve at the beginning of the fixation period. The dye diffuses down the axolemma of a small number of neurons within the tissue allowing microscopic visualization of the axon geometry without interference from connective tissue and other cells.

IMAGE PROCESSING AND ANALYSIS: Tissue sections mounted on microscope slides were imaged using a Nikon Diaphot TE300 inverted microscope. Images were acquired with Axon Imaging image acquisition hardware and software and a CCD camera. With a 40x objective lens, each 640x480 pixel image corresponded to 202x150 mm field. Some processing was necessary in order to automate the analysis of the images. The images are high contrast with the myelin of the axons stained dark blue and axoplasm not stained (white). The images can be easily segmented based on this contrast by a simple thresholding procedure. However, spatial variations in background staining or in field illumination must first be eliminated. This was accomplished by convolving the images with a large radius Gaussian image. This blurred image was then subtracted from the original to give an image with a uniform average intensity. After an approximate deconvolution step to sharpen the image and, therefore, the boundaries between axon and their myelin sheath, the images were thresholded at their mean intensity level. The resulting binary image showed axons as discrete approximately circular areas separate from each other and the background. An automated particle counting and measuring procedure was then performed giving the area, perimeter, and aspect ratio of the best-fit ellipse for each particle. Background areas with connective tissue that do not stain get counted along with the axons. However, these areas are irregularly shaped compared to the nearly circular axons. The Shape Index ($SI=4\pi A/P^2$, A = area, P = perimeter) indicates the how closely an area approximates a circle. For a circle, SI = 1. As the boundary becomes more irregular, the perimeter becomes large compared to the area, and the SI becomes smaller. This parameter was calculate for each particle, and those with a $SI < 0.65$ were rejected.

RESULTS

STRUCTURAL ANATOMY AND MECHANICS: The anatomy of the Guinea pig optic nerve is shown schematically in Figure 1 (Top). From the chiasm, where the two nerves cross before passing back to the visual cortex, the nerve curves to meet the optic foramen. It passes through the foramen at an angle of approximately 45° with respect to the cephalocaudal axis. Surrounding the

nerve between the globe and the optic foramen is a connective tissue sheath which is firmly attached to the skull at the foramen. Inside the skull, a connective tissue sheath surrounds the nerve and anchors it the to base of the skull. The total force applied to the nerve by pulling on the globe is balanced by the tension in the nerve itself, the parallel force in the connective tissue sheath between the globe and the foramen as well as tangential forces due to friction between the nerve and the sheath. Different values of this force are possible because the sheath inside the skull is relatively immobile whereas the sheath outside the skull may deform. This represents a statically indeterminate system.

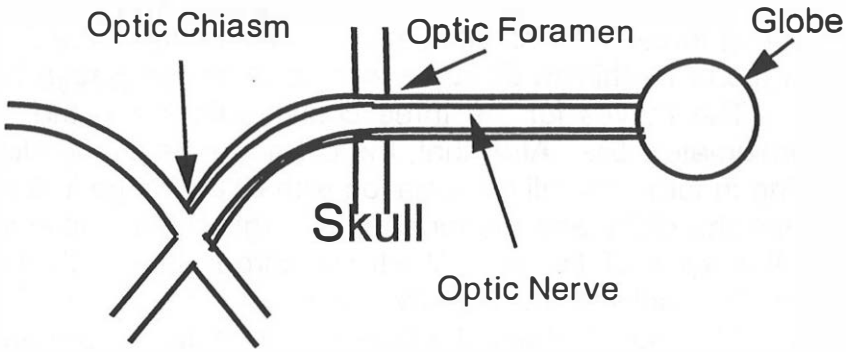

Figure 1. Schematic Anatomy of the Optic Nerve

Thus, in order to evaluate the relative contributions of the various components, three tests were performed in addition to the quasi-static loading of the intact

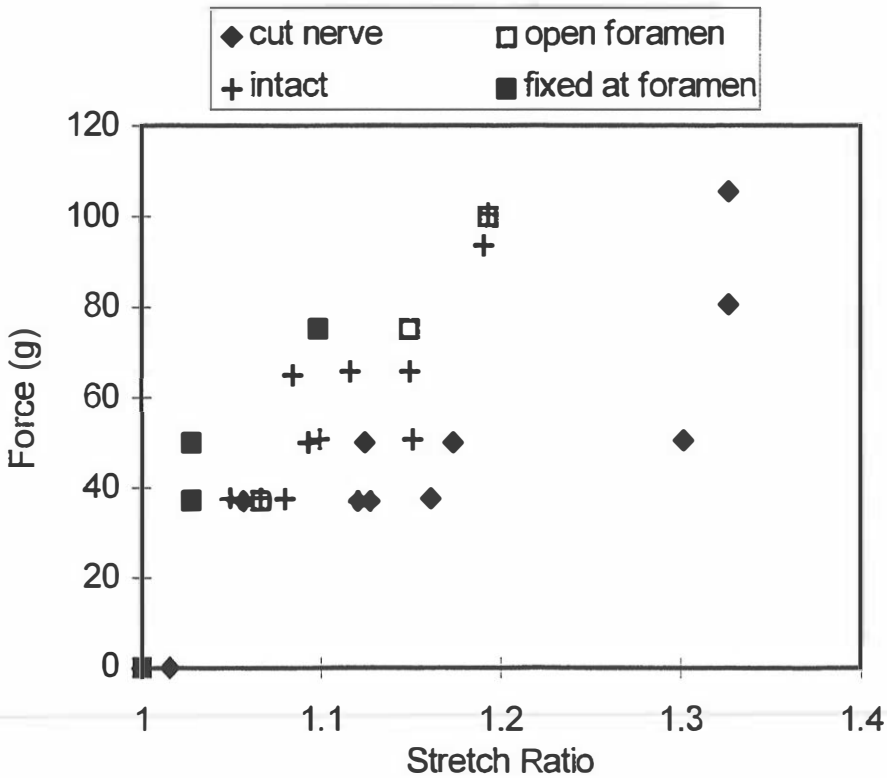

Figure 2. Force-deflection data for intact optic nerve structure and for various modified structures

composite structure. First, the nerve was dissected free from the foramen. This procedure effectively eliminates frictional forces since the sheath may now deform with the nerve such that no relative motion occurs; however, the parallel stiffness of the sheath may still contribute. The next modification tested was the severing of the nerve at the level of the chiasm. Thus, the forces resisting deformation are due to the stiffness of the sheath between the skull and the globe plus any frictional force due to the relative motion of the nerve within the sheath. The resulting force-strain relationships are plotted in Figure 2. In each case, the original globe to chiasm distance was used as the gauge length for strain calculation. The curves for the three configurations are the same for strains up to approximately 5%. After that, the cut nerve begins to slide within the sheath resulting in large overall deformation with little change in force. The connective between the globe and the foramen at large strains stiffens sharply as is typical of this type of tissue. At strains larger than 5%, the intact configuration and the isolated nerve have identical force-strain behaviors suggesting that in that range of strain, the parallel connective tissue bears very little load. To verify that the nerve itself bears most of the load, an additional experiment was performed. The final modification was to fix the nerve to the inner table of the skull at the foramen using superglue. Approximately 70% of the total length (globe to chiasm) of the nerve lies outside the skull. Thus, shortening the gauge length by 30% should increase the effective stiffness (using the globe to chiasm gauge length as before) accordingly. Indeed, Figure 2 shows the expected effect.

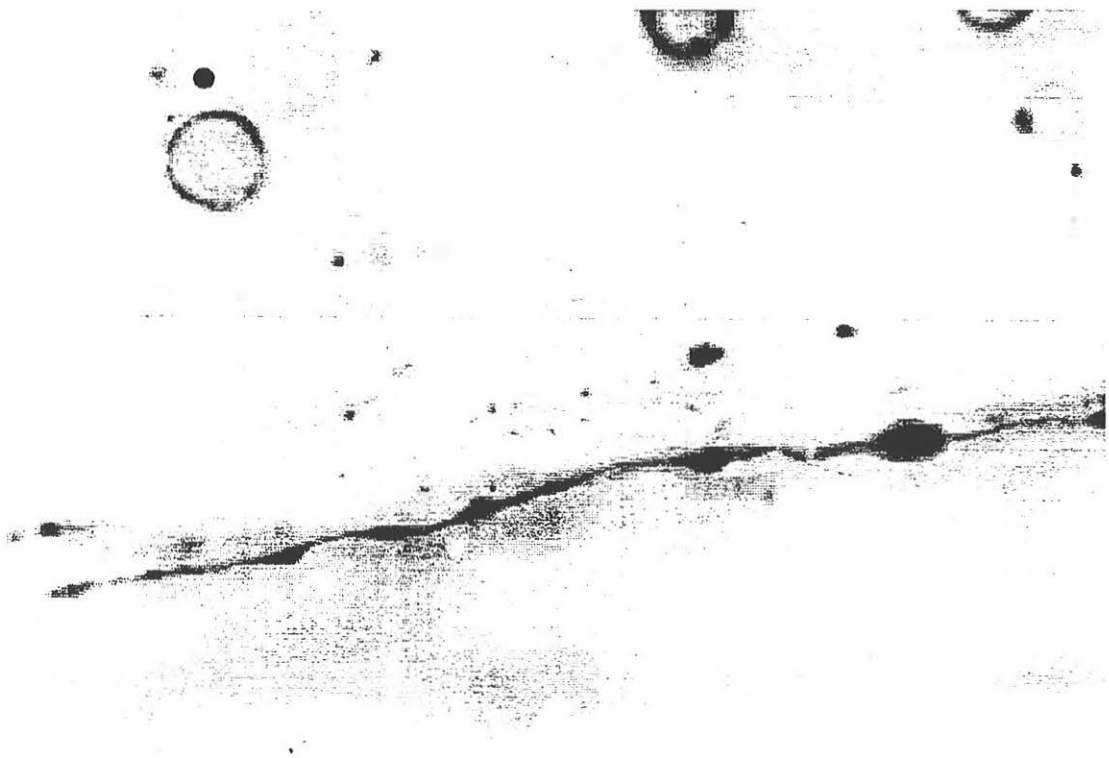

Figure 3 In Situ Geometry of an Individual Axon

MICROSTRUCTURAL ANATOMY: Histological sections revealed the presence of the connective tissue sheath described above. It was present even in what appeared to be "clean dissections." This finding prompted the mechanical studies above. We were also interested in the structure of individual axons within the tissue matrix. For this, the ordinary histological sections proved inadequate. A general waviness in the structure was observed in these sections and appeared to decrease with increasing levels of stretch; however, it was not possible to track individual axons for proper analysis.

The fluorescent tracer DiI was used to accomplish this aim. Figure 3 shows a typical fluorescence image obtained by this technique. This specimen was fixed in a relaxed state, i.e., no external force applied. Our experience has taught us that a cut nerve with no force applied will tend to shorten. Thus, axons of this specimen would be expected to be at least as wavy as in the unloaded nerve in vivo, if not slightly more wavy due to the contraction following cutting. In contrast to the impression from the histological sections, the individual axon appears to undulate only slightly with a much larger period and smaller amplitude than the waviness seen in brightfield images. Quantitative analysis of the waviness showed that the total length of the fiber divided by the end-to-end distance was only 1.02.

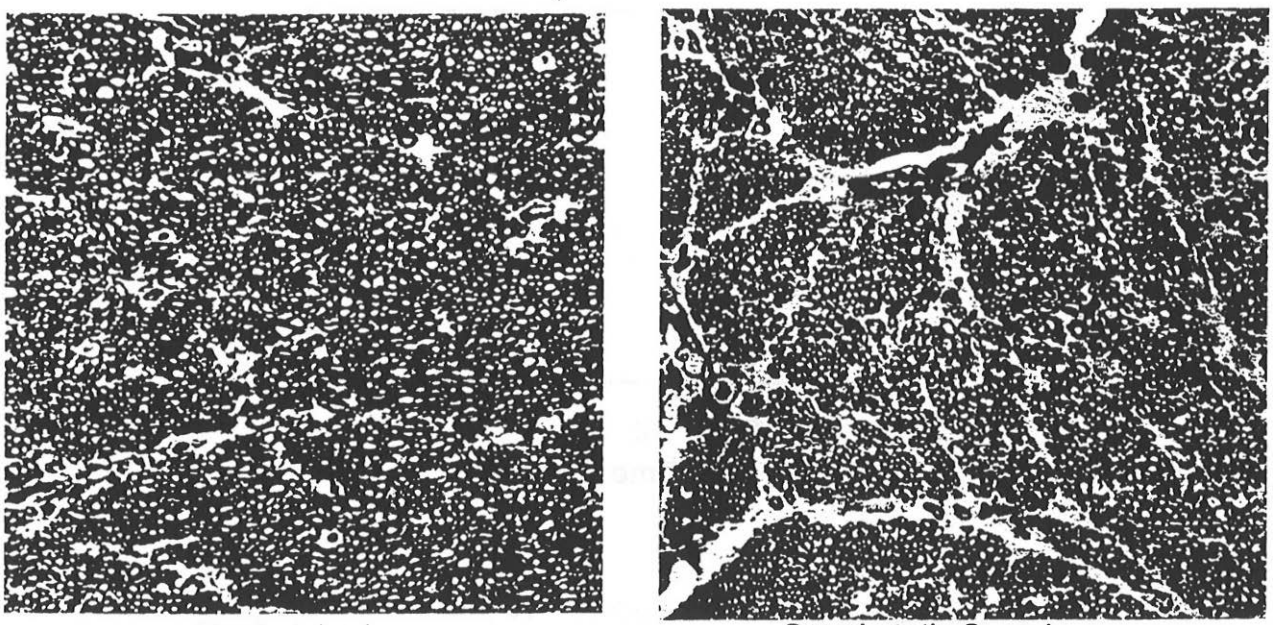

Unstretched Quasi-static Stretch

Figure 4. Control Optic Nerves

DYNAMIC LOADING: The cross section of the normal Guinea Pig optic nerve stained with toludine blue shows a large number of relatively uniformly sized axons (Figure 4, left). Furthermore, quasi-static loading as in the experiments described above has no effect on axonal morphology (Figure 4, right). Dynamic stretching of the optic nerve to 25 % (based on globe-to-chiasm length) causes a progressive swelling of axons that reaches a peak at 4 hours. The degree of

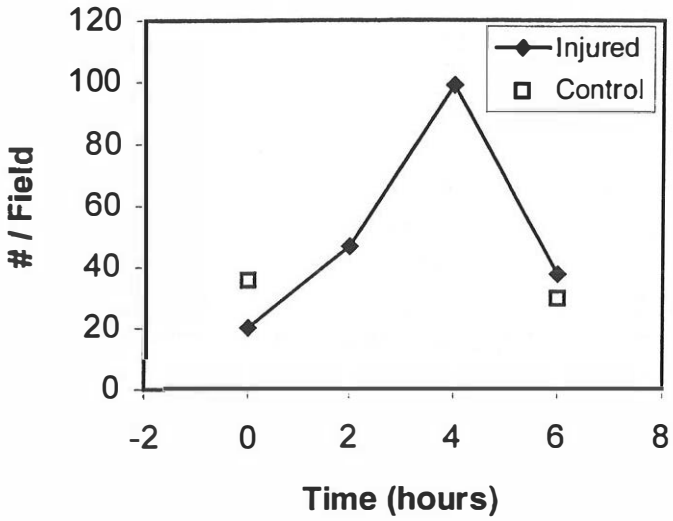

Figure 5 Number of Axons > 5 μm^2 per Field

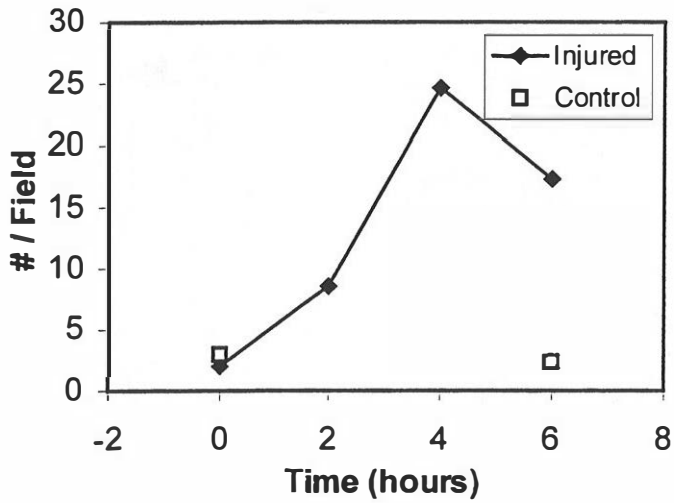

Figure 6 Number of Axons > 10 μm^2 per Field

swelling was characterized by counting the number of axons per microscope field that were greater than 5 μm^2 in cross-sectional area and the number that were greater than 10 μm^2 in area. Nerves fixed immediately following the stretch showed normal morphology. At all subsequent time points, the number of axons greater than 10 μm^2 was significantly higher than in unstretched controls and reached a peak value at 4 hours (Figure 5). The number of axons

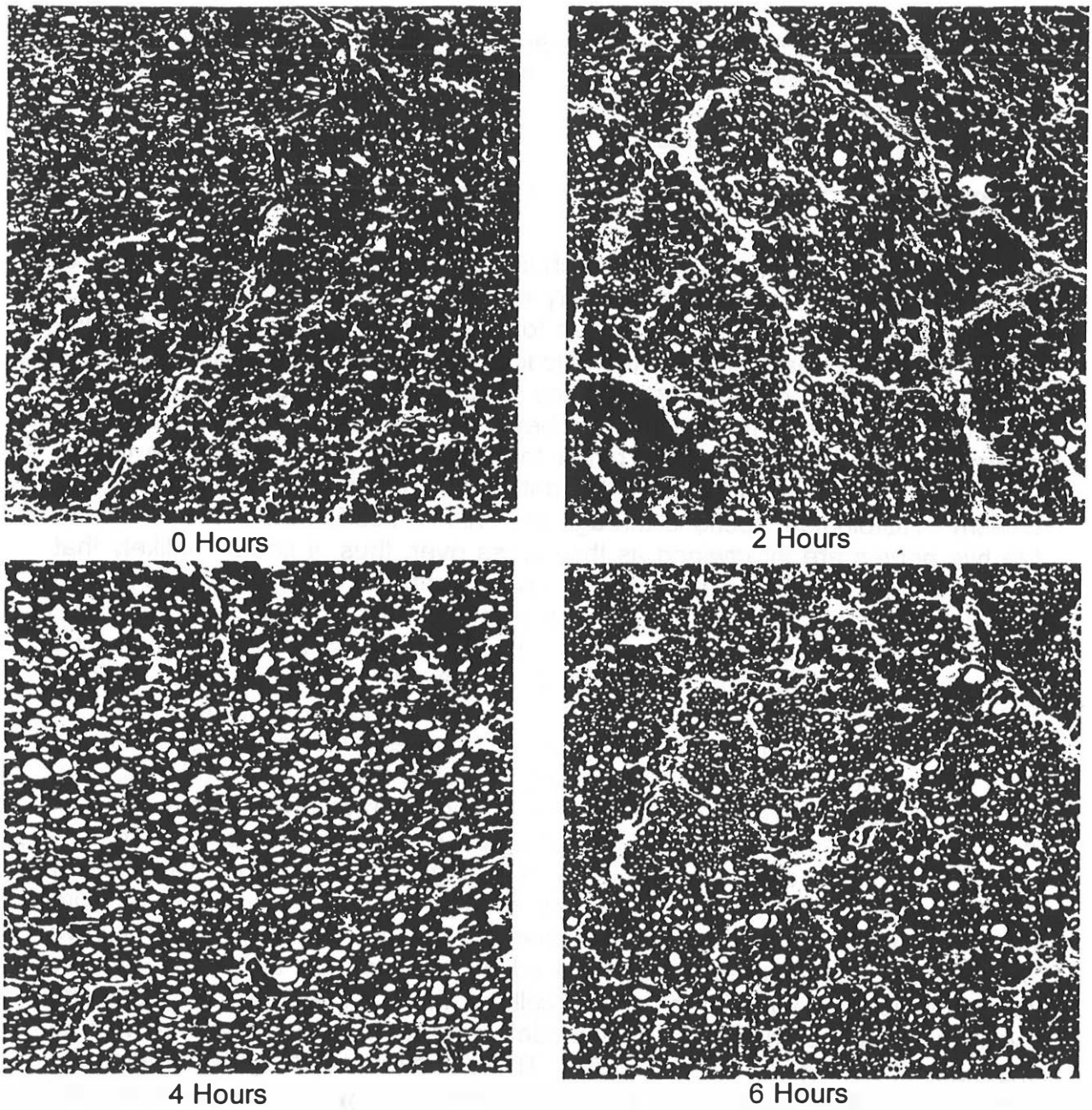

Figure 7. Injured Optic Nerve Sections

greater than 5 μm^2 was significantly greater only at the 4 hour time point (Figure 6). The six hour sham-operated control was not significantly different from the acutely fixed unstretched control. Figure 7 shows images representative of the data displayed in Figures 5 and 6.

DISCUSSION

We have taken measures to characterize and control the mechanical aspects of the optic nerve stretch injury model. These steps are essential for this model (or any other) to serve as a tool to establish neural injury tolerance criteria and to evaluate properly the efficacy of therapeutic strategies. We have demonstrated that displacement of the globe transits force throughout the length of the nerve to the chiasm and beyond. It appears that the nerve itself bears the majority of the stress rather than the associated connective tissue. The remaining uncertainty is in the nature of the end compliance, i.e. the chiasm. Histological sections through the chiasm itself show that axons from the two nerves are intertwined as they cross over, thus, it seems unlikely that there is slipping of nerves within the bundle. Therefore, we may assume that as long as the chiasm remains in place, we may regard it as a fixed end condition.

Using the information gained from these structural studies, we determined the appropriate pre-load to ensure dynamic and uniform deformation over the entire length of the nerve from globe to chiasm. The level of injury severity is therefore much greater than reported in previous models. This is evidenced by the severe swelling of axons that is easily detectable by light microscopy. Thus, this refined model should have greater utility since it does not require laborious electron microscopic examinations to be performed.

The time course of axonal swelling is consistent with earlier observations. The increased severity of injury should make this a more sensitive model for the detection of changes due to putative neuroprotective treatments. Our laboratory has focused its attention on the acute, primary mechanisms of neural injury at the cellular level. We feel that the acute swelling response in this in vivo model represents a primary response to mechanical damage to the axolemma. Thus, treatment strategies targeting the repair and stabilization of the cell membrane we are developing in our cell culture models, will subsequently be tested in this well-characterized in vivo model.

ACKNOWLEDGEMENTS: Funding for this project was provided by the CDC (R49CCR304684/5).

REFERENCES

Barbee, KA, Ford, CM, Blackman, BR, and Thibault LE Neural Cell Injury: Characterization and Treatment Strategy. Injury Prevention through Biomechanics 8:45-50 (1998).

Barbee, KA, Yazdi, J, Fijan, R, Croul, SE, and Thibault, LE. Basic Mechanics of the Guinea Pig Optic Nerve Strech Model for CNS Injury. Injury Prevention through Biomechanics 8:57-63 (1998).

Ellis, EF, McKinney, JS, Willoughby, KA, Liang, S, Povlishock, JT. "A new model for rapid stretch-induced injury of cells in culture: characterization of the model using astrocytes." J. Neurotrauma 12(3): 325-339 (1995)

Galbraith, JA, Thibault, LE, and Matteson, DR. "Mechanical and electrical responses of the squid giant axon to simple elongation." J. Biomech. Eng. 115: 13-22 (1993).

Gennarelli, T.A., Thibault, L.E., Tipperman, R., Tomei, G., Sergot, R., Brown, M., Maxwell, W.L., Graham, D.I., Adams, J.H., Irvine, A., Gennarelli, L.M., Duhaime, A.C., Boock, R., and Greenberg, J. Axonal injury in the optic nerve: A new model of mammalian central nervous system damage that simulates diffuse axonal injury in the brain. J. Neurosurgery, **71**: 244-250, 1989.

Jafari SS, Maxwell WL, Neilson M, Graham DI Axonal cytoskeletal changes after non-disruptive axonal injury. J Neurocytol 1997 Apr;26(4):207-21

Jafari SS, Nielson M, Graham DI, Maxwell WL Axonal cytoskeletal changes after nondisruptive axonal injury. II. Intermediate sized axons J Neurotrauma 1998 Nov;15(11):955-66

LaPlaca, M. C., and L. E. Thibault. An *in vitro* model of traumatic neuronal injury: loading rate-dependent changes in acute cytosolic calcium and lactate dehydrogenase release." J. Neurotrauma 14(6): 355-368 (1997).

Maxwell WL, Graham DI Loss of axonal microtubules and neurofilaments after stretch-injury to guinea pig optic nerve fibers. J Neurotrauma 1997 Sep;14(9):603-14

Maxwell WL, McCreath BJ, Graham DI, Gennarelli TA Cytochemical evidence for redistribution of membrane pump calcium-ATPase and ecto-Ca-ATPase activity, and calcium influx in myelinated nerve fibres of the optic nerve after stretch injury. J Neurocytol 1995 Dec;24(12):925-42